

Experience-Dependent Plasticity in S1 Caused by Noncoincident Inputs

David T. Blake, Fabrizio Strata, Richard Kempster, and Michael M. Merzenich

Coleman Laboratory and Keck Center for Integrative Neuroscience, University of California, San Francisco, California

Submitted 17 February 2005; accepted in final form 4 June 2005

Blake, David T., Fabrizio Strata, Richard Kempster, and Michael M. Merzenich. Experience-dependent plasticity in S1 caused by noncoincident inputs. *J Neurophysiol* 94: 2239–2250, 2005; doi:10.1152/jn.00172.2005. Prior work has shown that coincident inputs became corepresented in somatic sensory cortex. In this study, the hypothesis that the corepresentation of digits required synchronous inputs was tested, and the daily development of two-digit receptive fields was observed with cortical implants. Two adult primates detected temporal differences in tap pairs delivered to two adjacent digits. With stimulus onset asynchronies of ≥ 100 ms, representations changed to include two-digit receptive fields across the first 4 wk of training. In addition, receptive fields at sites responsive to the taps enlarged more than twofold, and receptive fields at sites not responsive to the taps had no significant areal change. Further training did not increase the expression of two-digit receptive fields. Cortical responses to the taps were not dependent on the interval length. Stimuli preceding a hit, miss, false positives, and true negatives differed in the ongoing cortical rate from 50 to 100 ms after the stimulus but did not differ in the initial, principal, response to the taps. Response latencies to the emergent responses averaged 4.3 ms longer than old responses, which occurs if plasticity is cortical in origin. New response correlations developed in parallel with the new receptive fields. These data show corepresentation can be caused by presentation of stimuli across a longer time window than predicted by spike-timing-dependent plasticity and suggest that increased cortical excitability accompanies new task learning.

INTRODUCTION

How does the brain change when we learn? The neural basis of experience-dependent plasticity encompasses a wide body of work in developmental and mature forms of plasticity. In all related studies, final functional representations are selected from a larger superset of initially available connectivity. In developmental plasticity in primary visual cortex, for example, thalamic axons grow into cortex and branch extensively. In an activity-dependent process, these extensive connections are pruned to a subset of their initial connectivity (Antonini and Stryker 1993; Crair et al. 1998). Here, we explore changes in functional representations in mature cortical areas to better understand their genesis.

In adult sensory cortex, suprathreshold responses are just the tip of the iceberg. Cell membrane recordings have verified that the subthreshold fields of sensory neurons are much broader than the suprathreshold fields (Fox 2002; Moore and Nelson 1998; Smits et al. 1991; Zarzecki et al. 1993). Simple perturbations in sensory exposure, such as synodactyly, result in enhancement of horizontal cortical connections (Smits et al. 1991; Zarzecki et al. 1993), and allow a functional remodeling of the hand representation that reflects the changes in hand use

(Allard et al. 1991). The emergence of multidigit receptive fields provides a model system for investigation of these phenomena. In normal animals, representational borders exist between digits so that typically no areas of primary somatic sensory cortex, or area 3b, have suprathreshold responses to more than one digit tip (Merzenich et al. 1978). Across these borders at distances of a few hundred microns, subthreshold inputs exist that are not expressed in the suprathreshold responses. Prior work (Wang et al. 1995) suggested that simultaneous stimulation of skin surfaces can convert these subthreshold responses to suprathreshold responses. Similar responses were not observed in the thalamic nuclei that provide the cortex with its input. Many questions remain about how these subthreshold responses become suprathreshold.

This study used cortical implants in adult owl monkeys to make daily observations on the development of these two-digit receptive fields. The behavior was constructed to test the range of relative input timings that can cause this form of plasticity. The range of time constants that cause reorganization has implications for reorganization in the human condition, for manual tasks such as typing, video games, and playing music, and may have importance in the generation of the pathological condition focal dystonia (Blake et al. 2002a). Cortical implants were used in the experimental design to document the emergent plasticity in spiking responses across daily training sessions (deCharms et al. 1999). In such an experiment, each electrode samples from the same cortical location before, during, and after task acquisition. The array allows sampling from the majority of the area 3b cortical columns involved in the behavior, and each electrode defines a daily sample from one column. Using such a highly controlled sample, brain changes caused by operant conditioning may be studied. In prior studies, animals were extensively trained, usually for several months, to be assured of observing any changes associated with the behavior in the acute, anesthetized, mapping studies. Using implants, this study observed the relevant time-course, phenomenology, and prevalence of suprathreshold two-digit receptive field development obtained in the awake behaving primate. Receptive field changes occurred concurrently with the behavioral changes, and the phenomenology suggests that cortical horizontal connections are a principal basis for the new receptive field components and that cortical excitability is increased by new task learning, as a mechanism that may complement spike-timing-dependent plasticity (STDP).

METHODS

Two adult owl monkeys were implanted in primary somatosensory cortex before behavioral training. The methods for the cortical implant

Address for reprint requests and other correspondence: D. T. Blake, 513 Parnassus Ave., S-877, San Francisco, CA 94143-0732 (E-mail: d Blake@phy.ucsf.edu).

The costs of publication of this article were defrayed in part by the payment of page charges. The article must therefore be hereby marked "advertisement" in accordance with 18 U.S.C. Section 1734 solely to indicate this fact.

have been described at length previously (deCharms et al. 1999). Briefly, implants consisted of a 7×7 square grid of microelectrodes with $350\text{-}\mu\text{m}$ spacing and were positioned into the cerebral cortex. After establishing an areflexic anesthetic level, primary somatosensory cortex was localized stereotaxically at 4 mm anterior to the interaural line and 14 mm lateral to the midline. A small burr hole was made for pilot recordings to verify expected somatotopy and to find the index finger representation. The implant was thus positioned on the representations of the index finger and an adjacent finger in area 3. Because of the microelectrode spacing and area of representations, 12 electrodes could be placed in distal fingertip representations that would respond to taps during the behavior. After several rounds of vertical repositioning during the first few weeks after the surgery to optimize recording depths, microelectrodes were not moved again, and the behavior was initiated. Recordings were made with parylene-insulated iridium microelectrodes (Micro Probe, Potomac, MD) with tip exposures between 5 and 7 μm long, chosen to maximize probability of sampling single units (Galambos and Davis 1943; Hubel 1957). This tip exposure also corresponds to 1–2 MOhms impedance tested at 1 kHz.

Figure 1A shows a rendering of the surface of the owl monkey brain with the expanded inset at the position of the hand in primary somatosensory cortex, area 3b (Kaas 2004). Microelectrodes were implanted across digits 2 (d2), 3 (d3), and 4 (d4) in the example taken from animal 1. Animal 2 was implanted across the representations of digits 1 and 2 (data not shown).

Behavior

Animals were trained in a holding task before the study. An animal began each trial by reaching its hand into a hand mold and contacting two motor tips. Each motor tip was instrumented with a gold-plated electrical contact detector, and a trial was initiated successfully if the animal placed two specific digits onto the motor tips. The animal, in the holding task, successfully completed a trial by maintaining contact for greater than one second. After successfully learning the holding task, and being implanted, the study began.

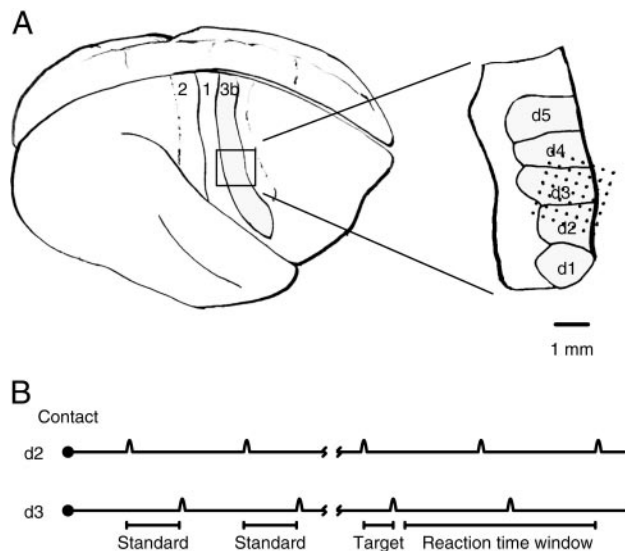


FIG. 1. *A*: implant location. *Left*: side aspect of the owl monkey brain. *Right*: anterior. Somatosensory strip in area 3b was implanted. *Inset*: approximate position of the 49 microelectrode implants in animal 1. Electrodes were implanted across the 2nd (d2), 3rd (d3), and 4th (d4) digital representations on the left hand. *B*: behavioral task. A trial began with an orienting response, the animal initiating contact with the tips of 2 motors. Then, 2 to 6 standard tap pairs were repeated. After the tap interval changed to the 100-ms target, which was shorter than the standard interval (200 ms), the animal could remove its hand and receive a reward.

TABLE 1. *Daily behavioral performance*

Day	Hit Rate 1	FP Rate 1	d' 1	Hit Rate 2	FP Rate 2	d' 2
1	0.30	0.29	0.03	0.21	0.15	0.23
2	0.21	0.25	-0.07	0.58	0.17	1.16
3	0.12	0.06	0.38	0.29	0.17	0.42
4	0.29	0.11	0.62	0.27	0.21	0.19
5	0.31	0.07	0.98	0.83	0.19	1.84
6	0.41	0.09	1.12	0.54	0.17	1.06
7	0.41	0.09	1.12	0.57	0.18	1.09
8	0.29	0.10	0.73	0.65	0.16	1.38

The behavioral task for the study, detecting a pattern of taps delivered to two fingers, is shown schematically in Fig. 1B. An animal began each trial by reaching its hand into a hand mold, contacting two motor tips, and sensing a series of tap pairs. Each tap was 100–150 μm in amplitude and had the shape of one cycle of an 80-Hz sinusoid, or 12.5 ms in length. The first tap was delivered to the index finger (d2), and the second to an adjacent finger: d3 for animal 1 and d1 for animal 2. The stimuli were initially separated by a standard interval of 200 ms. Stimulus pairs were separated by 500 ms. After two to six standard tap pairs, the interval length changed to the 100-ms target. All stimuli after the 100-ms target also had 100-ms intervals. An animal was correct in a trial (hit) if it removed its hand from the hand mold after the first presentation and before the third presentation of the target interval. Therefore the animal had to signal the change in interval length in the series. A miss occurred if the animal failed to remove its hand before the presentation of the third consecutive target in the series. A false positive occurred if the animal removed its hand at a potential target window, but before any target was presented. A true negative occurred if an animal failed to remove its hand at a potential target window in the absence of any target. Potential target windows followed the third, fifth, and seventh tap pairs presented in the series. If no target had been presented by the sixth standard, the seventh was always a target. Behavioral sessions preceded receptive field mapping. A correct trial resulted in a solenoid being triggered to release drops of dilute Tang for the animal.

Behavioral performance was assessed by comparing the probability of detecting the target, or the $\frac{\text{hit}}{\text{hit} + \text{miss}}$ ratio, with the probability of making a false-positive response in the same trial position. Determination that the animals used timing information to perform the task came from hit rates exceeding false-positive rates. Table 1 shows these rates averaged across the first two potential trial hit windows, as well as the d' values calculated using the standard normal distribution, for the first eight behavioral sessions for each animal. Hit rate 1 corresponds to the hit rate for animal 1 averaged across the first two potential target windows, and hit rate 2 corresponds to the averaged hit rate for animal 2. No trends for hit and false-positive rates were noted between the first two potential target windows.

Receptive field mapping

Mapping was possible because the animals were pretrained to present their hand to investigators. Probes with $\sim 1\text{-mm}$ -diam glass tips and a calibrated piezo-electric tapper were used to map. The tapper delivered a 12.5-ms smooth skin indentation from 0 to 30 μm in amplitude. Areas were considered part of the cutaneous receptive field if just visible indentation of the skin elicited a consistent response. Use of the piezo-electric tapper calibrated these measurements to be equivalent to roughly 15–20 μm of the brief taps in amplitude. Hairy, deep, Pacinian, and proprioceptive responses were also assessed. Most electrodes that sampled responses during the behavior were mapped successfully every study day for months.

The cortical implant was coupled to a Magnet data collection system (Biographics, Winston-Salem, NC). Thresholds were set for

each responsive microelectrode. Single units were also selected manually using an additional amplitude window and a low-amplitude threshold; 1.5 ms of the spiking waveform was saved for each threshold crossing. Off-line, single-unit quality was confirmed by a waveform analysis that used three criteria: signal-to-noise ratio, CV of maximal positive slope on the principal waveform deflection, and CV of maximal negative slope on the principal deflection. The signal-to-noise ratio, or the mean peak-to-peak magnitude divided by the noise SD, had to exceed five, and CVs for each unit had to be <0.25 . Multiunits were manually selected as single units but did not meet our single-unit statistical criteria. Times of trial initiation, tap delivery, and hand release were recorded in the same data stream as the spike waveforms.

All animal use was approved by the Institutional Animal Care and Use Committee at University of California, San Francisco.

Tap responses

Significant responses to taps were assessed using the responses to the 100-ms tap pairs, the target stimuli. For each day and each site, mean response rate and response SD were estimated from the 50 ms before the first tap onset using standard unbiased estimators. If the tap response in the 10- to 40-ms interval after tap onset exceeded 2.3 SD above the mean in at least three 1-ms bins, the response was considered significant. This statistical test has a single comparison probability of $P < 0.0037$, which is 30 choose 3 multiplied by a single bin $P < 0.0107$; 30 choose 3 is a probabilistic adjustment between a single bin probability and the probability of seeing this outcome in any 3 of 30 bins. This conservative single comparison probability allowed the per day experiment-wide chance of false identification to be $P < 0.05$. Comparisons were made for single- and multiunit data on all recorded channels each day. Receptive field components corresponding to the taps were confirmed with manual receptive field mapping.

Response latency

Response latency was assessed for every tap response found significant. The assessment was performed using a line intersection method (Friedman and Priebe 1998). The first line approximates the prestimulus rate. The second estimates the immediate poststimulus rate. Previous work (Friedman and Priebe 1998) has examined this method, and other methods, in detail, and found it to be robust and unbiased. Other methods, in particular estimations of the first data point significantly above background rate, are biased and problematic. This particular measure should correspond closely to the earliest time at which cortical action potentials are evoked by the stimulus.

Spike correlations

Tests for spike correlations were made between all recording pairs in which both sites had a significant response to at least one of the two taps. Two assessments were made. The first detects if the firing rates at two sites are related. It is equivalent to say that the firing rate at one of the two sites predicts the variability in firing rate at the second site. This correlation can be caused by a scaling of firing rate from trial to trial that is shared. For this reason we call this a cell assembly correlation.

Another measure of interest is a fine spike timing correlation that would indicate a high probability of two sites sharing an ionotropic connection. For example, the two sites may each receive a synapse from the same neuron or one of the two neurons may project to the other. Such sites will also test positively for a cell assembly correlation. The shape of the cell assembly correlation is predicted by the correlation of the average firing rates at each site. To be able to detect a fine spike timing correlation, the predicted correlation by the average firing rates was subtracted from the raw cross-correlogram,

and any remaining significant peaks indicate with high probability a shared ionotropic connection. These concerns are discussed at length in Brody (1998). A mathematical description of these methods follows.

Spike correlations were covariations between spike trains of two sites, say X and Y. These spike correlations exist beyond the correlations expected by chance, given the probability of spiking at each site. To calculate these spike correlations, the spike trains for each trial are represented in 1-ms bins with ones for each spike and zeros elsewhere. Let the spike train of trial n at site X be $S_X, n(t)$, where t is the time in units of milliseconds since the onset of the tap of interest. The peristimulus time histograms (PSTHs) from N trials is defined as

$$P_X(t) = \frac{1}{N} \sum_{n=1}^N S_{X,n}(t)$$

Next, the independent prediction of covariations was calculated from PSTHs at sites X and Y for offset times s between -20 and 20 ms

$$C_{\text{ind}}(s) = \sum_{t=0}^{100} P_X(t) \times P_Y(t+s)$$

which is proportional to the probability of a spike occurring in spike train X and a spike in train Y with an offset of s milliseconds, if the two spike trains were independent. C_{ind} defines how often coincident spikes occur by chance. It is also called the shuffle corrector, although it should be noted that the independent prediction contains correlations from the same trials as well as correlations between all pairwise combinations of other trials. With several hundred events used in the cross-correlation analysis, the difference between this shuffle predictor and the one described in Perkel et al. (1967) is quite small. This may be compared with the same trial-averaged cross-correlogram of the two spike trains

$$C(s) = \frac{1}{N} \sum_{n=1}^N \sum_{t=0}^{100} S_{X,n}(t) \times S_{Y,n}(t+s)$$

A departure of $C_{\text{ind}} - C$ from zero indicates that the two sites X and Y were not independent in spike generation. Significant differences between the independent prediction and the covariogram were assessed in 1-ms bins in which $C(s)$ exceeded $C_{\text{ind}}(s)$ by >3.4 SE ($P < 0.0003$). SE was set using the binary distribution with the spiking probability set as that found in the bin. The low probability P was set to correct for the large number of comparisons so that the experiment-wide probability of a false positive was $<5\%$. Although this statistical test does assess the lack of independence between two spike trains throughout a period of driven activity, slow covariations in excitability may also contribute to significance (Brody 1998). This test will be referred to as a test of membership in the same cell assembly, which means that trial-by-trial fluctuations in responsiveness are shared.

A more rigorous test was used to establish fine spike timing correlations which indicate high probability of shared ionotropic inputs or direct ionotropic projections between sites. For this test, the $C_{\text{ind}}(s)$ was shifted and scaled to match the $C(s)$. So, any slow covariations that would tend to scale the covariogram would be controlled for. Differences between the shifted and scaled independent prediction and the covariogram that exceeded the same statistical margin were considered significant.

RESULTS

Manually mapped receptive fields from each electrode exhibited a range of response types from day to day. Receptive fields grew and shrank, response strength waxed and waned,

and relative weighting of receptive field components changed. On this background of variability, the receptive fields defined on each electrode had elements that were invariant across the first weeks of training and elements that were variable, as seen in the maps of animal 1 in Fig. 2.

Although subsets of the receptive field remained stable in their location on the cutaneous receptor sheet throughout these 3- to 4-wk training periods, new receptive field components were, in many cases, added to existing fields. The two maps of animal 1 shown in Fig. 2 were separated in time by 16 days, or 12 behavioral sessions, and in that time, four sites developed significant responses to both taps used in the behavior. In both animals, two-digit receptive field development began to appear in the first week of the behavior. Two-digit sites had statistically significant spiking responses to both taps of the target stimulus in the behavior.

An example of receptive field change is shown in Fig. 3A. Receptive fields at this site always included a small patch of skin near the distal medial glabrous skin surface of the index finger distal phalanx. In addition to this invariant component, more proximal and lateral skin surface on the index finger were sometimes included, as well as lateral portions of the middle finger distal glabrous surface. This form of expansion was common, with skin surfaces adjacent to the invariant receptive field component being added to the receptive field.

In animal 1, 20 sites had field components that were conserved throughout training, and those 20 include all sites that had tap responses during the behavior. On average, 15 other sites had less reliable, but definable, spiking receptive fields on a training day. In animal 2, responses were less robust in

general, but 6 of the 11 sites that responded in the behavior had reliable and robust receptive field components, and the invariant portion of the initial receptive field remained a stable subset of all receptive fields recorded on that electrode throughout the training detailed in this report. The other five sites whose activity was modulated by the taps recorded somewhat less consistently, probably because of a change in the implant electronics between animals.

Receptive fields, defined daily in animal 1 before and after task initiation, expanded after the new behavior was introduced. Animal 2 receptive field data collection began with the behavior, so its receptive field data may not be compared with prebehavioral data. The receptive fields from each electrode were defined on the basis of the cutaneous receptive field or the portion of the skin surface with consistent responses to just visible skin indentations. In animal 1, there were nine sites with significant tap responses that also had predominantly cutaneous receptive fields every day. Another two channels with significant tap responses were not included. One had a consistent proprioceptive component and a variable cutaneous component of its receptive field, and the other had Pacinian input and lacked well-defined receptive field borders. For each of the nine sites, receptive field areas across a 6-wk period starting 2 wk before the task initiation were normalized to a within-site mean of one. This normalization prevented sites with larger receptive fields from dominating the change measures, as receptive fields in somatosensory cortex comprise a long-tailed distribution (DiCarlo et al. 1998). These nine sites increased in their receptive field areas in the 4 wk after behavior was initiated relative to the 2 wk before behavior was initiated

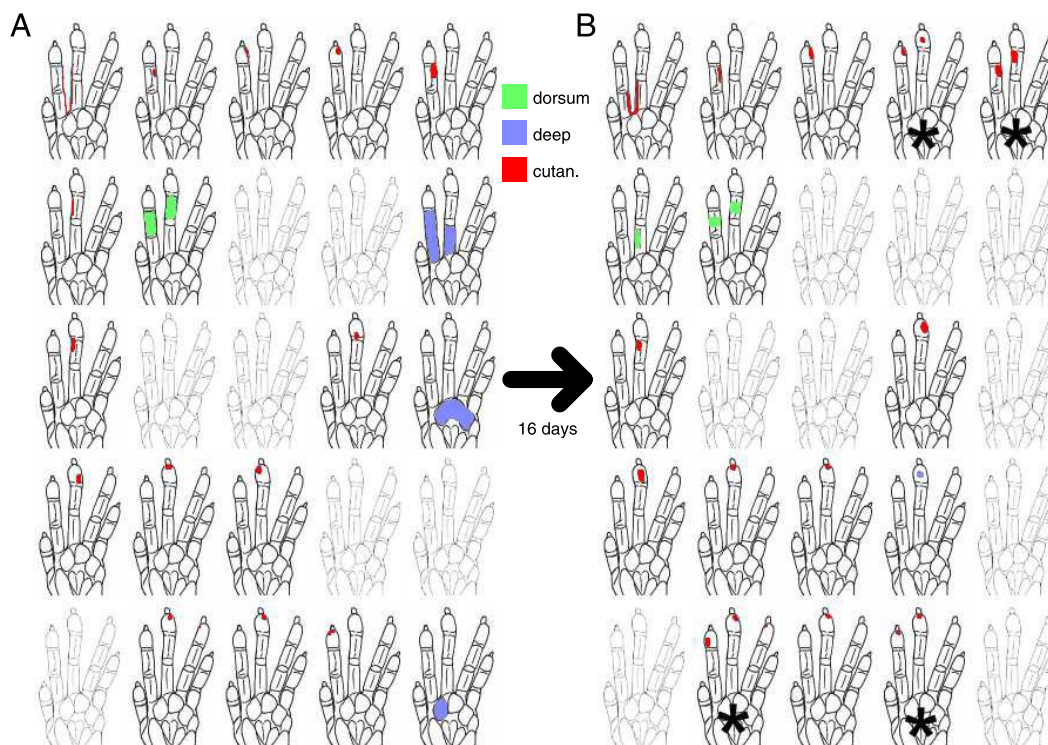


FIG. 2. Changes in the maps of somatosensory responses in animal 1. *A*: drawings of 25 receptive fields as mapped on a day before 2-digit receptive fields emerged. Spatial positions of the outlines of the monkey's left hand correspond to a 5×5 subset of the 49 electrodes of the implant. We surveyed cutaneous (red) and deep (blue) responses as well as responses on the dorsum (green). Gray hands indicate no determinable receptive field from that electrode on the day shown. *B*: receptive fields 16 days later. Twelve behavioral sessions separated *A* and *B*. *Sites where 2-digit receptive fields emerged. Recording sites are arranged in a $350\text{-}\mu\text{m}$ spacing grid. Anterior is right, medial is up.

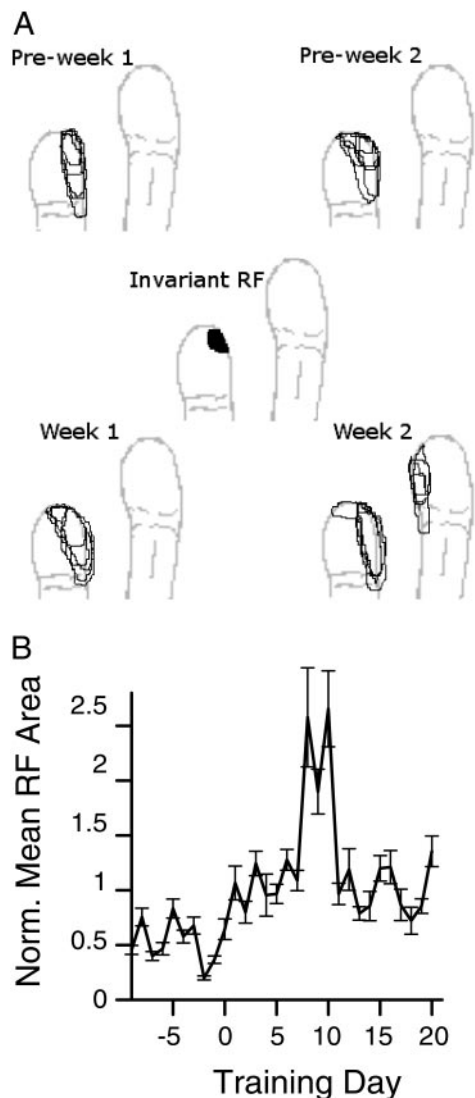


FIG. 3. Receptive field changes over time. *A*: receptive field maps from 1 site from 2 wk before the behavior was initiated and 2 wk after. Center plot shows the intersection of all 20 receptive fields. *B*: normalized receptive field area during training. Receptive field area from each site with a significant tap response was taken from 2 wk before training started to 4 wk after, and each site's areas were normalized to a within-site mean of 1. Average normalized areas across all sites that responded to the behavioral taps are shown. Areas were significantly larger after training began than before (t -test on normalized areas, $P < 10^{-7}$). Areas without significant tap responses had insignificant areal changes before and after behavioral initiation.

(t -test, $P < 10^{-7}$). The normalized averages, by week, were 0.58, 0.46, 0.94, 1.56, 1.29, and 1.04, and the daily averages across these nine channels are shown in Fig. 3*B*. At individual sites included in the nine sites, all sites had increases in the average receptive field area after task initiation, with a range from a 43% increase to a 300% increase and an average increase of 146%. In contrast, no significant change in receptive field area was found sampled across four sites that also had well-defined cutaneous receptive fields each day, but never had significant responses to the behavioral taps. These sites were intermixed spatially with the sites that had significant tap responses.

An example of multidigit receptive field development is shown in Fig. 4*A*. Single-unit responses were sampled across

four consecutive recording sessions from the same implanted microelectrode. A tap to the index finger began at *time 0*, and a tap to the third fingertip began at *time 100*. Single units sampled from this site developed statistically significant two-digit receptive fields on the fourth session shown. Multiunit mapping on the same electrode agreed with the single unit findings (data not shown). Figure 4*B* shows examples from spiking responses in the second animal, taken from one microelectrode across a 3-wk training epoch, with significant two-digit responses in the third week. Statistically significant tap responses had elevations in firing rate between 10 and 40 ms after tap onset, as detailed in METHODS.

Across all electrodes, the two-digit receptive field development progressed through 20 training sessions. Finally, two-digit fields were recorded at roughly 40% of sampled sites, as shown in Fig. 5*A*. The population statistics were compiled across all electrodes that yielded a significant response to either tap in the behavior relative to the prestimulus rates. The implants sampled 11 and 10 sites that responded to taps on the distal fingertips over cortical areas of roughly 2 mm² in each animal. Each animal was engaged in the behavior for >30 more training sessions after the initial 4-wk training period without further multidigit receptive field emergence.

The order-dependence of the formation of two-digit representations is shown in Fig. 5*B*, where the number of sites in which the responses to the first tap emerges in areas previously representing only the second tap (thin line) is smaller than in the converse case (thick line). Although we found five sites in which the responses to the second tap emerged in areas previously representing only the first tap, and only three sites for the converse, there is no significant impact of the order of stimulation on the emergence of new receptive field components. The nonsignificant trend favors responses to the second tap emerging in areas previously only responsive to the first tap.

To evaluate the coactivation time window to these stimuli, a histogram of the sum population response to the target stimulus taps was compiled. Figure 5, *C* and *D*, shows histograms from both animals. In these plots, neural responses recorded on all electrodes in one animal were added together. Approximately 50 ms of near-background activity separated the population responses to the two taps.

New responses at the eight sites with two-digit responses were equal or longer in latency than preexisting responses. The range was 0–7 ms. Two of the sites had latency differences of 0–2 ms, similar to the example in Fig. 6*A*. Five sites had latency differences of 4–7 ms, and the latency to the emergent response was longer. An example with longer latencies to the emergent response than to the initial response is shown in Fig. 6*B*. On these seven sites with two-digit responses, latency differences were conserved from day to day within 1 ms. The eighth site had highly stochastic responses and was judged poorly suited to latency analysis. The other seven sites had an average latency shift of 4.3 ms, significantly greater than zero (t -test, $P < 0.005$). Latency was the intersection of lines approximating prestimulus firing rate and poststimulus onset response (Friedman and Priebe 1998).

Neuronal responses to behaviorally categorized stimuli were analyzed. The categories were Hit, Miss, False Positive, and True Negative. Hit stimuli were the first two presentations of the target stimuli on correct trials. Miss stimuli were the first

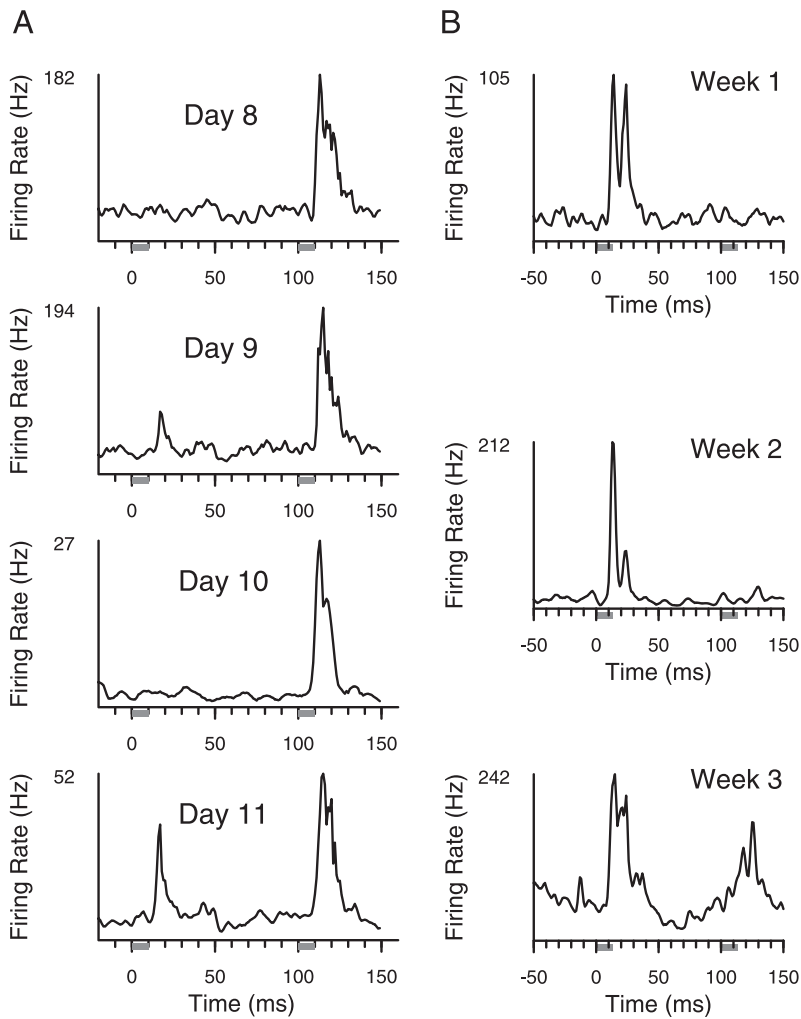


FIG. 4. Emergence of 2-digit receptive fields. *A*: sampled single-unit responses on 1 microelectrode in animal 1 over a 4-day period in which 2-digit responses emerged. Responses were defined across all 100-ms tap intervals delivered during the hold. A site had 2-digit responses if there were significant increments in firing rate, measured in action potentials per second, between 10 and 40 ms after a digit was tapped, relative to pretap activity. Gray bars indicate time that taps were delivered. *B*: sampled multiunit responses over 3 wk from 1 electrode in animal 2 showing the emergence of 2-digit receptive fields in the 3rd week.

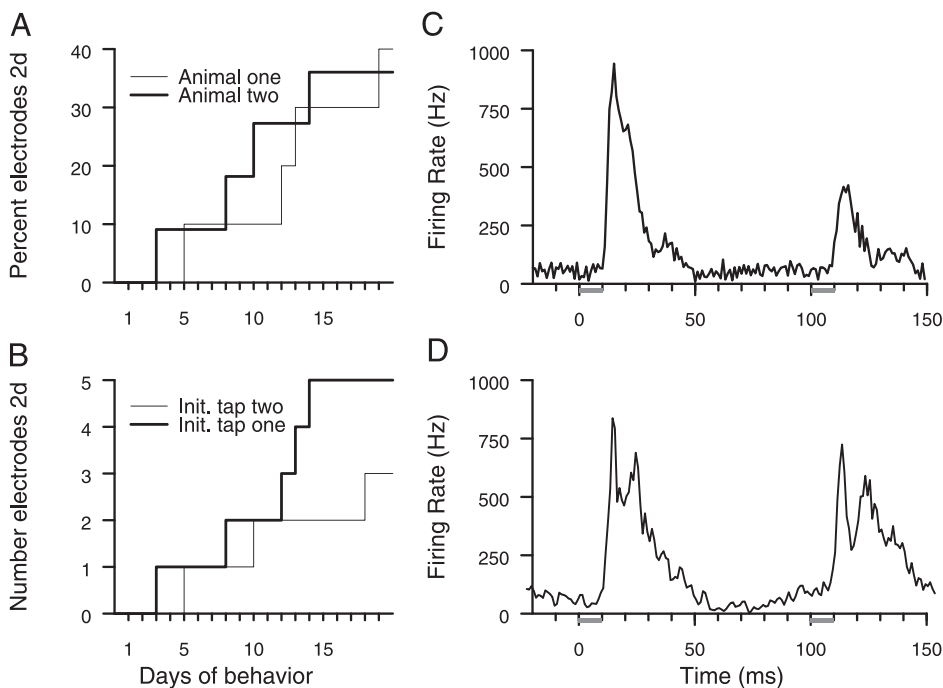


FIG. 5. *A*: cumulative plot of the percentage of sites that had 2-digit response properties. Thick line, development of 2-digit responses in 4 of 11 sites in animal 2; thin line, development of such responses in 4 of 10 sites in animal 1. Total number of sites used in plot includes all electrodes that sampled responses to either tap in any behavioral session. *B*: 2-digit receptive field development does not depend on order of taps. Same data as in *A* replotted to show sites that initially only responded to the 1st tap delivered to the index finger tip, but finally, after behavioral training, also had an emergent response to the 2nd tap at a different finger (thick line). Conversely, we also found sites that initially responded only to the 2nd tap, but finally had an emergent response to the 1st tap (thin line). *C*: population activity in animal 1. Sum of all sampled activity in response to target stimulus. Tap at *time 0* occurred on digit 2, and tap at *time 100* occurred on digit 3. *D*: population activity in animal 2. Tap at *time 0* occurred on digit 2, and tap at *time 100* occurred on digit 1.

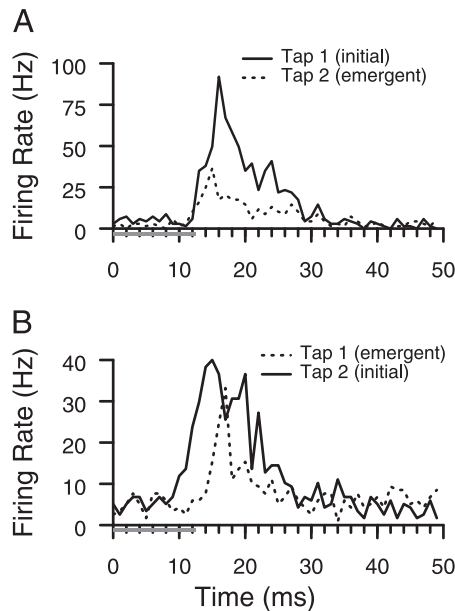


FIG. 6. Response latencies. Peristimulus time histograms (PSTHs) show responses to the 1st (Tap 1) and 2nd taps (Tap 2); taps (gray bars) and responses are aligned in time to allow for a better comparison of latencies. We compared responses that are present initially (solid lines) to emergent responses (dashed lines). *A*: example site in which latencies of the preexisting (solid) and the emergent (dashed) tap responses were identical. Before behavioral training, responses were sampled only to the 1st tap. *B*: example site in which latency of the emergent response (dashed) was about 5 ms longer than latency of the preexisting response (solid).

two presentations of the target stimuli on trials in which the animal failed to remove its hand within reaction time limits. False positive stimuli were long-interval, nontarget, stimuli that occurred in a potential target time window and were

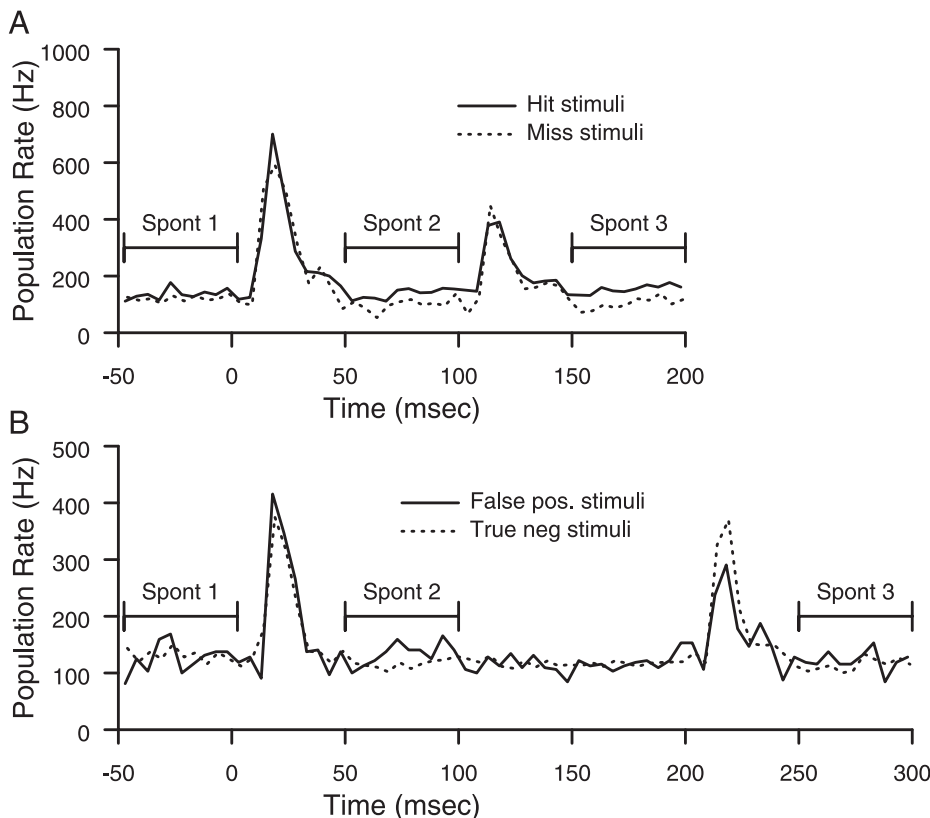


FIG. 7. Responses to different behavioral categories of trials. *A*: PSTH sum of all neuronal responses to the 1st 2 presentations of the target stimuli on hit and miss trials. *B*: PSTH sum of all neuronal responses, on a different day, to stimuli preceding false-positive and true-negative behavioral responses.

followed by the animal removing its hand. True negative stimuli were long-interval, nontarget, stimuli that occurred in a potential target time window that did not elicit a hand removal. Comparisons were done on firing rate in 50-ms time windows before the first tap, during the first tap, after the first tap, during the second tap, and after the second tap. No significant differences in the population responses during the taps were seen as a function of behavioral category.

The pre- and post-tap activity, however, followed different patterns based on type of stimuli. For convenience, we refer to these three periods as Spont 1, Spont 2, and Spont 3. Spont 1 is an average rate in the 50 ms before the first tap. Spont 2 is the average rate from 50 to 100 ms after the first tap onset. Spont 3 is the average rate from 50 to 100 ms after the second tap onset. The population response was defined as the sum of responses from all sites with a significant response to either tap. Comparisons were made, using sign tests, on whether the summed activity in the relevant time window was greater in one condition or another. Across 20 sessions, having a greater average response in 15 or more of those sessions would reach significance criteria ($P < 0.05$). Only effects that reach significance in both animals are included ($P < 0.0025$). On Hit trials, Spont 3 was significantly greater than Spont 2 and Spont 1. On Miss and True Negative trials, Spont 2 was significantly less than Spont 1, a finding not found on Hit and False Positive trials.

Figure 7 shows samples from 2 days that illustrates these trends in the data. In the behavioral session shown in Fig. 7*A*, the rates from the hit trial from 50 to 100 ms are greater than those in the miss trial, because the miss trial ongoing rates decrease after the first tap response. The difference increases after the second tap, from 150 to 200 ms, when the hit trial

PSTH ongoing rate increases. Figure 7B shows data from another day, to show the decreases in rate after the first tap in a True Negative response, but not in a False Positive response. The average decrease in miss trials between Spont 1 and Spont 2 was 3.8% in animal 1 and 3.2% in animal 2. The average increase in hit trials from Spont 2 to Spont 3 was 4.2% in animal 1 and 11.0% in animal 2. The average decrease between Spont 1 and Spont 2 on True Negative responses was 8.1% in animal 1 and 7.1% in animal 2.

Evidence for conversion of the tap interval length into a rate code was not found. Across all sites with significant responses to the second tap, average spike counts were compared between the shorter and longer intervals. A sample plot is shown in Fig. 8A. The data shown had a significant response to each tap. The responses to the second taps at different interval lengths are very similar to each other, but time-shifted. In Fig.

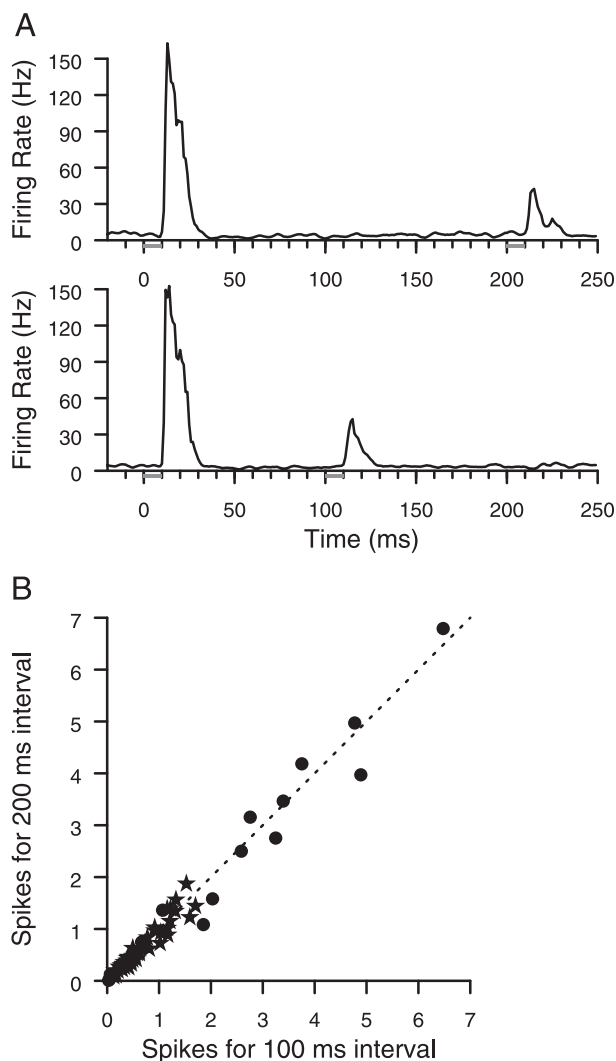


FIG. 8. Responses do not depend on the tap intervals. *A*: firing rate histograms of responses from neurons at a 2-digit site to taps at 100- and 200-ms intervals. *B*: population data showing strength of all significant neural responses to 2nd taps of 200-ms intervals compared with responses to 2nd taps of 100-ms intervals. No significant effects of interval length on response to 2nd taps were found using sign or *t*-test. Stars, data from animal 1; circles, data from animal 2; line, prediction if the 2 responses are equal. Each data point shows integral of response PSTH after subtracting prestimulus rate for the 2 conditions. This number is averaged over all daily trials.

8B, the magnitudes of the responses to second taps at interval lengths of 100 and 200 ms are compared, and across the population, the trend is for responses to be similar independent of interval length.

To determine if responses in new representations were synchronized with older, preexisting ones, spike timing correlations were also tracked over the course of behavioral training. Such correlations indicate statistical relationships between the time of spikes in two neurons that would be expected if the neurons shared ionotropic input or if one neuron projected to the other. Initially, in both animals, such correlations were only found between pairs of neurons that responded to the taps on the same finger. These spike timing differences were always within 3 ms of synchronous, and the two neurons were always separated by 700 μm or less.

As the new two-digit representations emerged, spike timing correlations emerged across distances $\leq 1,400 \mu\text{m}$, which indicated that spike timing correlations came with changes in representational structure. Typical properties of emergent spike timing correlations are shown in Fig. 9. In the example, one site, X, responded only to the index finger either in mapping, or in the behavior. Site Y responded primarily to the thumb, but had an emergent representation of the index finger. The correlation shown in Fig. 9B was during the responses to taps on the shared representation, the index finger, and this correlation spanned a horizontal cortical distance of 1.26 mm. Spike-timing correlations were not common (10 of 405 in animal 1, 9 of 45 pairs in animal 2, correlations were tested between all pairwise combinations in which both recordings contained at least 1 significant tap response) and were almost always synchronized within 1 ms (17 of 19 cases). The indication is that shared spike timing, synchrony, may be present between a site with an emergent representation of a digit and a second site representing that digit, just as it may be present between two sites initially sharing a representation.

Analysis of spike correlations to establish membership in cell assemblies was also performed (see METHODS), because two sites may covary in their response strength from trial to trial, without implying direct connections that are shared. In both animals, initial cell assembly correlation was prevalent between pairs that had significant responses to the same taps. In addition, cell assembly correlation across digital representations emerged at three of eight sites before two-digit receptive fields were recorded and were present in seven of eight sites by the day two-digit receptive fields developed. Cell assembly correlations were more common than fine spike timing correlations (60 of 405 pairs in animal 1, 21 of 45 pairs in animal 2). The distribution of distances at which cell assembly correlations were found in the first and last 3 days of the behavior are shown in Fig. 9C. There is a significantly increased probability of two sites having cell assembly correlations at the end of training compared with the beginning (sign test, $P < 0.05$), and the increased probability of correlation predominantly occurred at distances from 1 to 2 mm.

DISCUSSION

One-digit receptive fields were converted to two-digit receptive fields across 3 to 4 wk of behavioral training at a cross-digit interval discrimination task. The two-digit receptive fields occurred in roughly 40% of the population. The two-digit fields

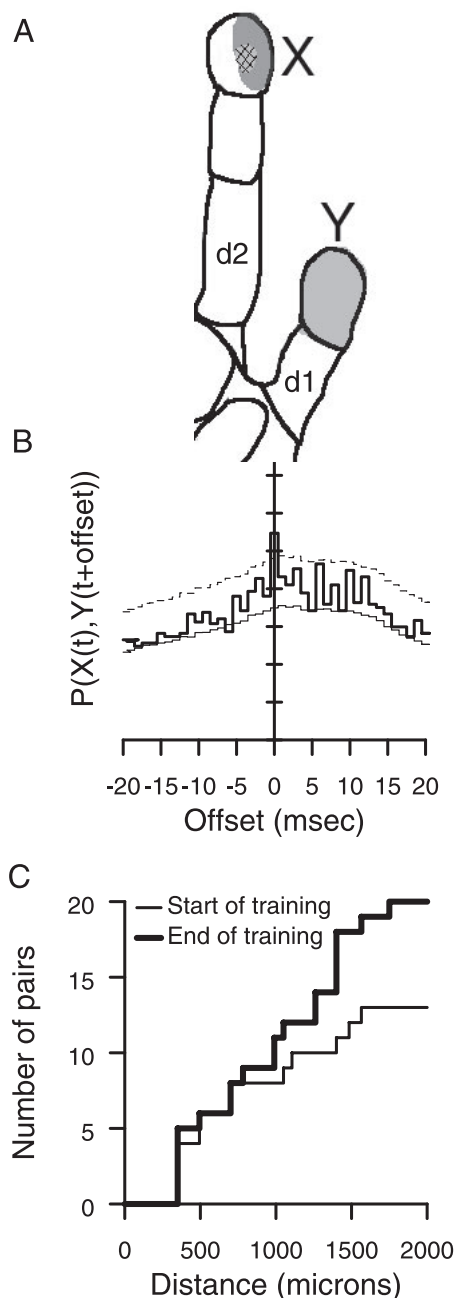


FIG. 9. Spike correlations. *A*: cutaneous spiking receptive fields from sites X and Y in animal 1. Distance between microelectrodes is 1.26 mm. Light-shaded receptive field was measured at site Y; dark-shaded receptive field was measured at the tip of d2 was measured at site X. Cross-hatched receptive field is shared. *B*: cross-correlation between X and Y during tap on index finger. Thin line, independent prediction; thick line, actual covariation; dashed line, single bin significance threshold for $P < 0.0003$. Elevated covariation at time 0 is significant for fine spike timing correlations. *C*: spatial distribution of cell assembly correlations in both animals. In the 1st 3 training sessions (thin line) there were fewer correlated pairs than in the last 3 training sessions (thick line).

appeared equally prevalent at sites that initially responded to the first tap on the index finger and sites that initially responded only to the second tap on an adjacent finger. Receptive field areas at sites responding to the taps more than doubled in the first 4 wk after task initiation. The emergent digital responses occurred with longer latencies than the original receptive field components. The strength of the second tap responses were not

dependent on interval length. Correlations during tap responses were initially restricted in spatial scale, but broadened out so that new correlations were established as new receptive field components formed.

Evidence for recoding of interval length, or time, into neural activity was not found, which suggests that the mechanisms involved in cortical temporal processing are dissociated from the receptive field reshaping mechanisms. The response strength to second taps occurring after a 200-ms interval was not statistically different from the response strength to second taps occurring after 100-ms intervals. The responses appeared indifferent to changes in interval length. Neural networks in nonneocortical areas are capable of sensitivity to this range of intervals (Buonomano and Merzenich 1995; Buonomano et al. 1997). Primary somatosensory cortex, area 3b, does perform such a transform for intervals in the range of 20–60 ms (Hernandez et al. 2000), and similar results exist in primary auditory cortex (Lu et al. 2001). Time processing in sensory systems may occur at different sites in the CNS depending on the interval length (Merzenich et al. 1993). The lack of temporal processing of stimuli that became co-represented suggests a dissociation between the origins of synaptic change via STDP and the synaptic change related to reinforcement. This difference has been noticed before (Shulz et al. 2003).

The behaviorally determined differences in ongoing cortical activity after the taps were delivered shows that expectation has an influence on cortical state. After the first tap, response ongoing rates are generally decreased, unless the animal was preparing to make a motor response for false positives or hits. Only if the animal was preparing for a hit did the ongoing rates increase after the second tap response. Preparation of a motor response was matched in false positive and hit stimuli, but only hit stimuli were associated with reward. Other studies have found a signal reflecting an animal's decision process in association cortices (Mountcastle 1993; Romo et al. 2002; Shadlen and Newsome 2001). Our finding of increased ongoing rate after the first tap on hit and false-positive trials compared with true-negative and miss trials suggests an element of preparedness modulates the excitability of primary somatic sensory cortex, independently of the decision process. The increased activity after the second tap of the target stimulus may be a reflection of a decision process that the animal expects to lead to reward.

The available evidence, most before this study, suggests that the locus for this class of adult experience-dependent cortical plasticity is cortical in origin. A prior study of multidigit receptive fields in owl monkey S1 found no multidigit correlate in the thalamus, the level just below primary sensory cortex in the ascending pathway (Wang et al. 1995). A similar parallel is drawn in the rat whisker barrel system where whisker trimming, a nonpathological manipulation, causes representational cortical plasticity not observed in the thalamus (Wallace and Fox 1999a,b). Intracellular cortical studies in which experimentally induced digital fusion used to cause multidigit receptive fields in raccoons (Smits et al. 1991; Zarzecki et al. 1993) provide evidence for a substrate for this plasticity in horizontal cortico-cortical connections. In the cases in which an animal is forced to adopt a new sensori-motor use of its hand or whiskers, the adaptation process forces learning and its associated reinforcement on the animal. In our study, natural reinforcers were offered on completion of behavioral trials. It is worth

noting that mechanisms are demonstrably different in the case of nerve injuries (Wall et al. 2002). The limited evidence on changes in response latency in our study is consistent with the results from an intracellular study of experimentally induced digital syndactyly (Zarzecki et al. 1993), which found some overlap in response latencies for emergent and original inputs, but found an average latency shift of 7 ms, and made a compelling argument that cortical horizontal connections are strengthened as an underlying mechanism.

Cross-correlational analysis detects a linear dependence in neuronal activity between pairs of recordings. In this study, we segregated between two types of cross-correlations. An insightful theoretical work (Brody 1998) showed that the standard cross-correlational analysis (Perkel et al. 1967) produced significant results if the two sites share covariance from trial-to-trial, without any other source of linear dependence. For example, if the animal hand positioning caused a 5% change in responsiveness from trial-to-trial, sites responding to the same taps could show a cross-correlational peak without sharing connections. The cross-correlational peak would characteristically take the shape of the convolution of the independent responses. We termed this a "cell assembly correlation" to imply that the neurons shared some common input, but not necessarily shared first-order connectivity. In our study, the prevalence of this type of correlation increased, and this increase occurred almost entirely at distances of 1–2 mm, larger than those in the classic cortical column (Mountcastle 1957; Powell and Mountcastle 1959). In turn this implies that the representational cortical column, or horizontal distance across which overlapping activity may be detected, is malleable with behavioral training in adults.

A goal of cross-correlational analysis not served by this type of statistical finding is the detection of connectivity. We have provided a conservative method to control for cell assembly correlations which finds cross-correlations not explicable by slow covariations in rate. These were termed "fine spike timing" correlations. Using this method, correlated neurons separated by distances of $\leq 1,400 \mu\text{m}$ were found after the task learning, which implies neurons across these distances shared connections.

The phenomenology of the behaviorally driven emergence of two-digit receptive fields places constraints on the mechanisms that could have caused it. We consider first the possibility that STDP is the principal mechanism at work. STDP causes presynaptic activity followed by postsynaptic activity to lead to synaptic strengthening, and postsynaptic activity followed by presynaptic activity to lead to synaptic weakening. The difficult case to explain is the emergence of the responses to the second tap in the representation of the first tap. Neurons in the first tap initial representation are strongly activated, and 55–100 ms later receive subthreshold inputs that become suprathreshold over the first weeks of the behavior. Those inputs should become depressed, and not enhanced, by STDP in neurons that initially respond to the first tap (Bi and Poo 1998; Debanne et al. 1998; Egger et al. 1999; Feldman 2000; Koester and Sakmann 1998; Markram et al. 1997; Zhang et al. 1998).

In a second scenario, consider the possibility that two-digit responses occur as repeated behavioral reinforcement caused subthreshold inputs, in general, to become suprathreshold. Data in other sensory systems suggest that acetylcholine, a neuromodulator known to be triggered by behavioral reinforce-

ment (Richardson and DeLong 1990), causes cellular changes that would make subthreshold inputs suprathreshold (Woody et al. 1978), and stimulation of ascending pathways that include the cholinergic systems causes spiking changes as though subthreshold inputs became suprathreshold (Singer 1979). Intracellular recording and digit manipulations have shown that digital inputs in normal animals cause subthreshold responses in adjacent representations (Hickmott and Merzenich 1998; Smits et al. 1991; Zarzecki et al. 1993). A mechanism by which this circuitry is unmasked when reinforcement increases cortical excitability would powerfully augment STDP mechanisms in determining the steady state cortical map (Fregnac and Shulz 1999). Our finding that receptive field area doubles and that receptive fields appear to add peripheral components to an invariant receptive field core specifically support the hypothesis that new task learning causes increases in cortical excitability. It is worth noting that the animals were engaged in the holding behavior before the task initiation. In this holding behavior, the animals made contact with the two probes with the two operant digits. This contact was, on average, substantially larger in skin indentation than the 100- to 150- μm taps delivered to the digits after task initiation. This small change in mechanical stimulation, accompanied by a large change in reinforcement contingencies, caused the increased cortical excitability noted in mapping. Increased BOLD functional MRI has also been found after visual task learning (Schwartz et al. 2002), and our previous work has shown a change in the sensory response to stimuli associated with reinforcement (Blake et al. 2002b).

A role for reinforcement in complementing known synaptic plasticity processes implies that reinforcement is critical for this plasticity. A good argument to support this hypothesis comes from a pair of crossover studies (Recanzone et al. 1992a,b). Animals were presented with both somatosensory and auditory stimuli, and rewarded for correctly responding to only one sensory modality. Cortical map plasticity was only seen in the sensory cortex associated with the task reinforcement. The other sensory modality, stimulated but not rewarded, remained not obviously different from control animals. Further evidence for the impact of reinforcement in causing plasticity in mature animals comes from comparing sensory exposure based plasticity in immature and mature animals. In mature animals, sensory exposure has caused short-term plasticity (Dragoi et al. 2000; Fu et al. 2002; Godde et al. 2000; Yao and Dan 2001) that lasts from tens of minutes to a few hours, but does not last for days. In immature animals, acoustic exposure without reinforcement can cause plasticity (Zhang et al. 2002).

Similar plasticity is not expressed in mature animals exposed to the same stimuli. The available evidence suggests that exposing adults to nonreinforced sensory stimuli does not cause the same magnitude or sort of changes in cortical representation that reinforced stimuli cause, or that nonreinforced exposure causes in developing animals. These results, and previous experiments on adult representational changes in sensory cortex due to behavior (Blake et al. 2002b; Buonomano and Merzenich 1998; Cruikshank and Weinberger 1996), are all consistent with the hypothesis that once an animal learns that stimuli will precede a reinforced motor action, the representations of those stimuli are strengthened relative to others through mechanisms involving strengthening of intracortical

synaptic connections and endogenous release of neuromodulators caused by association with reinforcement.

Whereas previous studies used longer training periods and single observation time points to assess how the brain changes in operant conditioning (Jenkins et al. 1990; Recanzone et al. 1992a,b; Wang et al. 1995; Xerri et al. 1996), this study watched it occur over a several week period. Further training did not result in strengthening of these effects. The results support the view that the sensory cortex maintains a long-term base of stability through its thalamocortical connections, and changes little in functional representations from consistent day-to-day experience. Significant behavioral change, specifically in the relation between reinforcers and sensory inputs, causes functional plasticity that is cortical in origin and tracks the behavioral change. Increases in cortical excitability probably act to gate endogenous synaptic plasticity processes. Whereas the behaviors may not be ethological to these species, they represent basic forms of spatio-temporal integration well within the range of normal experience. The length of time the animals perform the behavior matters less than the behavioral changes on adopting operant training, and the parallel neural changes shortly thereafter.

ACKNOWLEDGMENTS

J. Medina, D. Polley, and R. Ramachandran provided useful commentary on the manuscript. We thank D. Moorman and S. Desai for participating in data collection for these experiments. Technical assistance in this project was provided by K. MacLeod, L. Bocskai, K. McGary, and M. Fong.

Present address for R. Kempster: Institute for Theoretical Biology, Humboldt Universität Berlin, Berlin, Germany.

GRANTS

This work was supported by the Coleman Fund, HRI, the Sooy Fund, and National Institute of Neurological Disorders and Stroke Grants 1F32NS-10154 and NS-10414. F. Strata was supported by Human Frontier Science Program Organization long-term Fellowship LT 00743/1998-B. R. Kempster was supported by Deutsche Forschungsgemeinschaft Grant Ke 788/1-1.

REFERENCES

- Allard T, Clark SA, Jenkins WM, and Merzenich MM. Reorganization of somatosensory area 3b representations in adult owl monkeys after digital syndactyly. *J Neurophysiol* 66: 1048–1058, 1991.
- Antonini A and Stryker M. Rapid remodeling of axonal arbors in the visual cortex. *Science* 260: 1819–1821, 1993.
- Bi G and Poo M. Synaptic modifications in cultured hippocampal neurons: dependence on spike timing, synaptic strength, and postsynaptic cell type. *J Neurosci* 18: 10464–10472, 1998.
- Blake D, Byl N, Cheung S, Bedenbaugh P, Nagarajan S, Lamb M, and Merzenich M. Sensory representation abnormalities that parallel focal hand dystonia in a primate model. *Somatosens Motor Res* 19: 347–357, 2002a.
- Blake DT, Strata F, Churchland AK, and Merzenich MM. Neural correlates of instrumental learning in primary auditory cortex. *Proc Natl Acad Sci USA* 99: 10114–10119, 2002b.
- Brody CD. Slow covariations in neuronal resting potentials can lead to artefactually fast cross-correlations in their spike trains. *J Neurophysiol* 80: 3345–3351, 1998.
- Buonomano DV, Hickmott PW, and Merzenich MM. Context-sensitive synaptic plasticity and temporal-to-spatial transformations in hippocampal slices. *Proc Natl Acad Sci USA* 94: 10403–10408, 1997.
- Buonomano DV and Merzenich MM. Temporal information transformed into a spatial code by a neural network with realistic properties. *Science* 267: 1028–1030, 1995.
- Buonomano DV and Merzenich MM. Cortical plasticity: from synapses to maps. *Annu Rev Neurosci* 21: 97–102, 1998.
- Crair M, Gillespie D, and Stryker M. The role of visual experience in the development of columns in cat visual cortex. *Science* 279: 566–570, 1998.
- Cruikshank S and Weinberger N. Evidence for the hebbian hypothesis in experience-dependent physiological plasticity of neocortex: a critical review. *Brain Res Brain Res Rev* 22: 191–228, 1996.
- Debanne D, Gahwiler B, and Thompson S. Long-term synaptic plasticity between pairs of individual CA3 pyramidal cells in rat hippocampal slice cultures. *J Physiol* 507: 237–247, 1998.
- deCharms RC, Blake DT, and Merzenich MM. A multielectrode implant device for the cerebral cortex. *J Neurosci Methods* 93: 27–35, 1999.
- DiCarlo JJ, Johnson KO, and Hsiao SS. Structure of receptive fields in area 3b of primary somatosensory cortex in the alert monkey. *J Neurosci* 18: 2626–2645, 1998.
- Dragoi V, Sharma J, and Sur M. Adaptation-induced plasticity of orientation tuning in adult visual cortex. *Neuron* 28: 287–298, 2000.
- Egger V, Feldmeyer D, and Sakmann B. Coincidence detection and changes of synaptic efficacy in spiny stellate neurons in rat barrel cortex. *Nat Neurosci* 2: 1098–1105, 1999.
- Feldman D. Timing-based LTP and LTD at vertical inputs to layer II/III pyramidal cells in rat barrel cortex. *Neuron* 27: 45–56, 2000.
- Fox K. Anatomical pathways and molecular mechanisms for plasticity in the barrel cortex. *Neuroscience* 111: 799–814, 2002.
- Fregnac Y and Shulz D. Activity-dependent regulation of receptive field properties of cat area 17 by supervised Hebbian learning. *J Neurobiol* 41: 69–82, 1999.
- Friedman H and Priebe C. Estimating stimulus response latency. *J Neurosci Methods* 83: 185–194, 1998.
- Fu Y, Djupsund K, Gao H, Hayden B, Shen K, and Dan Y. Temporal specificity in the cortical plasticity of visual space representation. *Science* 296: 1999–2003, 2002.
- Galambos R and Davis H. The response of single auditory nerve fibers to acoustic stimulation. *J Neurophysiol* 6: 39–58, 1943.
- Godde B, Stauffenberg B, Spengler F, and Dinse H. Tactile coactivation-induced changes in spatial discrimination performance. *J Neurosci* 20: 1597–1604, 2000.
- Hernandez A, Zainos A, and Romo R. Neuronal correlates of sensory discrimination in the somatosensory cortex. *Proc Natl Acad Sci USA* 97: 6191–6196, 2000.
- Hickmott P and Merzenich M. Single-cell correlates of a representational boundary in rat somatosensory cortex. *J Neurosci* 18: 4403–4416, 1998.
- Hubel DH. Tungsten microelectrode for recording from single units. *Science* 125: 549–550, 1957.
- Jenkins WM, Merzenich MM, Ochs MT, Allard T, and Guic-Robles E. Functional reorganization of primary somatosensory cortex in adult owl monkeys after behaviorally controlled tactile stimulation. *J Neurophysiol* 63: 82–104, 1990.
- Kaas J. Evolution of somatosensory and motor cortex in primates. *Anat Rec A Discov Mol Cell Evol Biol* 281: 1148–1156, 2004.
- Koester H and Sakmann B. Calcium dynamics in single spines during coincident pre- and postsynaptic activity depend on relative timing of back-propagating action potentials and subthreshold excitatory postsynaptic potentials. *Proc Natl Acad Sci USA* 95: 9596–9601, 1998.
- Lu T, Liang L, and Wang X. Temporal and rate representations of time-varying signals in the auditory cortex of awake primates. *Nat Neurosci* 4: 1131–1138, 2001.
- Markram H, Lubke J, Frotscher M, and Sakmann B. Regulation of synaptic efficacy by coincidence of postsynaptic APs and EPSPs [see comments]. *Science* 275: 213–215, 1997.
- Merzenich MM, Kaas JH, Sur M, and Lin CS. Double representation of the body surface within cytoarchitectonic areas 3b and 1 in “SI” in the owl monkey (*Aotus Trivirgatus*). *J Comp Neurol* 181: 41–73, 1978.
- Merzenich M, Schreiner C, Jenkins W, and Wang X. Neural mechanisms underlying temporal integration, segmentation, and input sequence representation: some implications for the origin of learning disabilities. *Ann NY Acad Sci* 682: 1–22, 1993.
- Moore C and Nelson S. Spatio-temporal subthreshold receptive fields in the vibrissa representation of rat primary somatosensory cortex. *J Neurophysiol* 80: 2882–2892, 1998.
- Mountcastle VB. Modality and topographic properties of single neurons of the cat’s somatic sensory cortex. *J Neurophysiol* 20: 408–434, 1957.
- Mountcastle VB. Temporal order determinants in a somesthetic frequency discrimination: sequential order coding. *Ann NY Acad Sci* 682: 150–170, 1993.
- Perkel DH, Gerstein GL, and Moore GP. Neuronal spike trains and stochastic point processes. II. Simultaneous spike trains. *Biophys J* 7: 419–440, 1967.

- Powell TP and Mountcastle VB.** Some aspects of the functional organization of the cortex of the postcentral gyrus of the monkey: a correlation of findings obtained in a single unit analysis with cytoarchitecture. *Bull Johns Hopkins Hosp* 105: 133–162, 1959.
- Recanzone GH, Merzenich MM, and Jenkins WM.** Frequency discrimination training engaging a restricted skin surface results in an emergence of a cutaneous response zone in cortical area 3a. *J Neurophysiol* 67: 1057–1070, 1992a.
- Recanzone GH, Merzenich MM, Jenkins WM, Grajski KA, and Dinse HR.** Topographic reorganization of the hand representation in cortical area 3b owl monkeys trained in a frequency-discrimination task. *J Neurophysiol* 67: 1031–1056, 1992b.
- Richardson RT and DeLong MR.** Context-dependent responses of primate nucleus basalis neurons in a go/no-go task. *J Neurosci* 10: 2528–2540, 1990.
- Romo R, Hernandez A, Zainos A, Lemus L, and Brody C.** Neuronal correlates of decision-making in secondary somatosensory cortex. *Nat Neurosci* 5: 1217–1225, 2002.
- Schwartz S, Maquet P, and Frith C.** Neural correlates of perceptual learning: a functional MRI study of visual texture discrimination. *Proc Natl Acad Sci USA* 99: 17137–17142, 2002.
- Shadlen M and Newsome W.** Neural basis of a perceptual decision in the parietal cortex (area LIP) of the rhesus monkey. *J Neurophysiol* 86: 1916–1936, 2001.
- Shulz D, Ego-Stengel V, and Ahissar E.** Acetylcholine-dependent potentiation of temporal frequency representation in the barrel cortex does not depend on response magnitude during conditioning. *J Physiol Paris* 97: 431–439, 2003.
- Singer W.** Central-core control of visual cortex functions. In: *The Neurosciences, Fourth Study Program*, edited by Schmitt FO and Warden FG. Cambridge, MA: MIT Press, 1979, p. 1093–1109.
- Smits E, Gordon D, Witte S, Rasmusson D, and Zarzecki P.** Synaptic potentials evoked by convergent somatosensory and corticocortical inputs in raccoon somatosensory cortex: substrates for plasticity. *J Neurophysiol* 66: 688–695, 1991.
- Wallace H and Fox K.** Local cortical interactions determine the form of cortical plasticity. *J Neurobiol* 41: 58–63, 1999a.
- Wallace H and Fox K.** The effect of vibrissa deprivation pattern on the form of plasticity induced in rat barrel cortex. *Somatosens Mot Res* 16: 122–138, 1999b.
- Wall J, Xu J, and Wang X.** Human brain plasticity: an emerging view of the multiple substrates and mechanisms that cause cortical changes and related sensory dysfunctions after injuries of sensory inputs from the body. *Brain Res Brain Res Rev* 39: 181–215, 2002.
- Wang X, Merzenich MM, Sameshima K, and Jenkins WM.** Remodelling of hand representation in adult cortex determined by timing of tactile stimulation. *Nature* 378: 71–75, 1995.
- Woody C, Swartz B, and Gruen E.** Effects of acetylcholine and cyclic gmp on input resistance of cortical neurons in awake cats. *Brain Res* 158: 373–395, 1978.
- Xerri C, Coq JO, Merzenich MM, and Jenkins WM.** Experience-induced plasticity of cutaneous maps in the primary somatosensory cortex of adult monkeys and rats. *J Physiol* 90: 277–287, 1996.
- Yao H and Dan Y.** Stimulus timing-dependent plasticity in cortical processing of orientation. *Neuron* 32: 315–323, 2001.
- Zarzecki P, Witte S, Smits E, Gordon D, Kirchberger P, and Rasmusson D.** Synaptic mechanisms of cortical representational plasticity: somatosensory and corticocortical EPSPs in reorganized raccoon SI cortex. *J Neurophysiol* 69: 1422–1432, 1993.
- Zhang L, Bao S, and Merzenich M.** Disruption of primary auditory cortex by synchronous auditory inputs during a critical period. *Proc Natl Acad Sci USA* 99: 2309–2314, 2002.
- Zhang L, Tao H, Holt C, Harris W, and Poo M.** A critical window for cooperation and competition among developing retinotectal synapses. *Nature* 395: 37–44, 1998.